A Method for Predicting Pile Bearing Capacity From Dynamic Penetration Tests

F. Schnaid, M.J. Langone

Abstract. This paper presents a new method for predicting the axial capacity of piles from dynamic penetration tests which is based on the concepts of soil dynamics and principles of energy conservation. The energy delivered to the hammer-rod-sampler system and transferred to the soil is computed from the numbers of blow counts N_{spt} and is analytically converted in a penetration dynamic force. The dynamic force allows the unit resistance mobilized in the SPT sampler (model) to be determined, which is then used to predict the unit resistance mobilized in a prototype pile. The strong direct relationship between the ultimate resistance of driven steel piles and the SPT dynamic force, without any bias of soil type, validates the method. Extension of the method to other pile types requires empirical parameters to account for installation effects. Predictions of 89 instrumented static pile load test database demonstrate that the proposed methodology can be efficiently used in the assessment of axial pile capacity, providing a practical way of increasing reliability in pile design by accounting for effects controlling dynamic penetration.

Keywords: pile analysis, bearing capacity, penetration tests, energy conservation.

1. Introduction

The prediction of pile bearing capacity can be achieved using different methods of analysis such as interpretation of data from full-scale pile load tests, dynamic analysis and testing based on wave equations, static analysis based on soil properties and static analysis using the results of in situ tests. Given to the fact that penetration tests are used worldwide as the primary index test for site characterization, traditional methods of pile analysis and design often rely on empirical approaches based on SPT and CPT data (*e.g.* Bustamante & Giasenelli, 1982; Ruiter & Beringen, 1979; Aoki Velloso, 1975). These methods may produce inaccurate responses and unreliable predictions, because pile design depends on soil stratigraphy, pile characteristics, driving and installation methods, drainage and loading conditions. Applicability is therefore restricted to the database upon which the method has been developed and tested, and local experience and engineering judgment still plays an important role in pile analysis and design.

Among existing approaches, those established on the bases of SPT results receive severe criticism for their empirical nature, simplified assumptions, scattered predictions and discrepancies between predicted and measured loads. Although considerable literature is available on this matter, there is no single method of pile design based on dynamic penetration that has some theoretical background other than statistical.

Previous efforts have been made to estimate an average static resistance mobilized during sampler penetration (Schmertmann; 1979; Aoki *et al.*, 2004). An alternative method for the interpretation of dynamic penetration tests was proposed by Odebrecht *et al.* (2005) and Schnaid *et al.* (2008) from which the energy delivered to the rod string is used to calculate a dynamic force that represents the soil reaction to the penetration of the SPT sampler (F_d). Lobo (2007) used this dynamic force to develop an approach for predicting the axial bearing capacity of piles and Lobo *et al.* (2009) demonstrated the applicability of the approach by comparing measured and predicted ultimate loads from a database of 272 full scale load tests. Langone (2012) presented an independent assessment based on the interpretation of results from fully instrumented pile load tests. These results are presented in this paper and are used to validate a method for estimating the axial capacity of vertically loaded isolated piles.

2. Theoretical Developments

The proposed approach is based on the concepts of soil dynamics and principles of energy conservation. By computing the total energy delivered to the soil, Odebrecht *et al.* (2005) demonstrated that the potential energy (PE_{h+r}) has to be expressed as a function of the nominal potential energy (E^*), permanent sampler penetration ($\Delta\rho$) and weight of both hammer and rods, as well as three efficiency coefficients designed to account for energy losses during the energy transference process:

$$PE_{h+r} = \eta_3 \left[\eta_1 (0.75 + \Delta\rho) M_h g + \eta_2 \Delta\rho M_r g\right] \qquad (1)$$

where M_h is the hammer weight; M_r the rod weight; g the gravity acceleration; and η_1, η_2 and η_3 the efficiency coefficients. The nominal potential energy E^* represents a part of

Fernando Schnaid, PhD, Associate Professor, Departamento de Engenharia Civil, Universidade Federal do Rio Grande do Sul, Porto Alegre, RS, Brazil. e-mail: fernando@ufrgs.br.
Marcelo Júlio Langone, MSc, Civil Engineering, Petrobras Transporte S.A., Rio de Janeiro, RJ, Brazil. e-mail: marcelolangone@hotmail.com.
Submitted on April 9, 2012; Final Acceptance on March 1, 2013; Discussion open until August 30, 2013.

the hammer potential energy to be transmitted to the soil. An additional hammer potential energy is given by $M_h\, g\, \Delta\rho$ and the other part is transmitted by the rod potential energy $M_r\, g\, \Delta\rho$ which cannot be disregarded for tests carried out at great depths in soft soils, *i.e.* conditions in which $\Delta\rho$ and M_r are significant. Equation 1 requires a previous calibration of efficiency coefficients, which as a preliminary estimate for Brazilian SPT configurations can be assumed as $\eta_1 = 0.76$; $\eta_2 = 1$ e $\eta_3 = (1\text{-}0.0042l)$, where l is the total rod length, (Odebrecht *et al.*, 2005). Note that η_3 is adimensional, so the number before l has a m^{-1} dimension.

Since Eq. 1 gives the energy effectively delivered to the soil, with all losses accounted for by means of the efficiency coefficients, it is in principle possible to use this potential energy to calculate the mean dynamic reaction force (F_d) applied to the soil during sampler penetration (Schnaid *et al.*, 2007; Schnaid *et al.*, 2004; Schnaid, 2005):

$$F_d = \frac{\eta_3\eta_1(0.75M_hg) + \eta_3\eta_1(\Delta\rho M_hg) + \eta_3\eta_2(\Delta\rho M_rg)}{\Delta\rho} \qquad (2)$$

The sampler-soil interaction model is therefore represented by a dynamic mean reaction force that is calculated from the work produced by the non-conservative forces derived from the potential energy produced by the hammer-rod-sampler system.

The dynamic force F_d can now be used as an input value to compute the pile axial load by combining bearing capacity theory to the principles of cavity expansion. The ultimate axial load capacity of the pile (Qu) is the sum of two components: the end-bearing capacity (Q_P) and the shaft friction capacity (Q_L), which can be expressed as:

$$Q_u = Q_P + Q_L = A_p q_p + U\int_0^L f_l\, dL = A_p q_P + U\sum f_{l,i}\Delta L \qquad (3)$$

where q_p is the unit end bearing resistance, f_l local shaft friction, U the perimeter of the pile, A_p the area of the pile base and ΔL a pile length segment. Unlikely the cone, where the tip resistance q_c shows strong correlation with q_p and f_l, the dynamic force F_d has to be interpreted in order to estimate these two variables. Interpretation does not include specific considerations regarding the drainage paths around the penetrating sampler.

2.1. End-bearing

Estimating end bearing requires specific considerations regarding the mode of penetration of the sampler. Ideally a simple inspection of the soil plug inside the sampler is sufficient to identify whereas plugged or unplugged penetration has taken place at the depth of the pile tip. However this is not done in current investigation practice and, for the sake of simplicity, the proposed method was developed for piles embedded in stiff soils where sampler penetration is generally plugged (implying that floating piles would require different treatment). Plugged penetration is an assumption of the proposed methodology; other assumptions can be made within the same framework of energy propagation and energy conservation principles leading to slightly different results.

In a plugged penetration mode, the dynamic force is the sum of two terms: shaft friction and end-bearing resistance. By combing bearing capacity to cavity expansion (Vésic, 1972) it is possible to calculate the relative contribution of these two terms for a set of typical parameters. Use of Vésic's formulation follows recommendations from Eurocode 7 (1997) and API RP2A (2000). A parametric analysis demonstrates that end-bearing corresponds to 60% to 80% of the measured penetration force (Lobo *et al.*, 2009) which justifies considering the SPT bearing resistance $q_{p,spt}$ as 70% of the total measured penetration force:

$$q_{p,spt} = \frac{F_{d,p}}{a_p} = \frac{0.7F_d}{a_p} \qquad (4)$$

being a_p the area of the sampler base ($\pi 5.1^2/4 = 20.4$ cm^2).

Extrapolating measurements from penetration tests to real scale pile load test data is therefore a direct process that is not biased by soil conditions, pile length (L), pile diameter (D) and pile aspect ratio (L/D). In doing so, a recommendation is made to calculated F_d from the average N value taken in the zone of 2.0 pile diameters (D) above and below the pile tip, which is consistent to previously reported studies in both SPT and CPT interpretation data (*e.g.* Bazaraa & Kurkur, 1986; Briaud & Tucker, 1988; Xu & Lehane, 2005).

2.2. Shaft friction

The shaft friction calculated by the SPT ($f_{l,spt}$) is simply the dynamic force divided by the inner and outer areas of the sampler, expressed as:

$$f_{l,spt} = \frac{F_d}{a_l} \qquad (5)$$

being a_l the area of the sampler shaft. In this case, friction components mobilized inside and outside the sampler are considered to be the same. This assumption has been numerically evaluated by Lobo (2010) and it is believed to reproduce the basic mechanism that takes place during penetration in soft and loose materials.

The measured values of $f_{l,spt}$ can then be integrated along depth to estimate the actual pile shaft, and by doing so a number of simplified considerations are necessary:

i the sampler shaft friction has been shown to be much greater than the actual pile shaft friction due to what has been generally recognized as scale effects. These effects need to be considered when extrapolating measurements from penetration tests to real scale pile load test data, as already established by previous interpretation methods using SPT and CPT results (*e.g.* De

Ruiter & Beringem, 1979; Bustamante & Gianeselli, 1982). Lobo *et al.* (2009) proposed reducing $f_{l,spt}$ by a factor of 0.2 based on a comprehensive analysis comprising 271 real scale pile load tests. Della Rosa (2009) observed scale effects of the same other of magnitude when performing tests using SPT with diameters ranging from 3.6 to 7.2 cm. Langone (2012) confirmed these observations when interpreting instrumented pile load tests;

ii the shaft friction developed on a pile in tension is smaller than that mobilized by a pile loaded in compression (*e.g.* Lehane *et al.*,1993; de Nicola & Randolph (1993); Jardine *et al.*, 2005; Lehane *et al.*, 2007). This effect is not considered in the current analysis which implies that the predicted friction resistance corresponds to a pile loaded in compressions and should be reduced for a pile under tension;

iii in driven piles, the shaft capacity is known to habitually increase with time (*e.g.* Axelsson, 1998; Jardine *et al.*, 2005a; Lehane *et al.*, 2005a. Data considered in the present analysis generally represents long term conditions where installation effects have been partially settled;

iv strains in the pile that have been mobilized before the start of the test due to residual load must be considered, and in cases where these values are reported the residual loads were adjusted before establishing the true load distribution (*i.e.* the true load is, mainly, the sum of the installation load distribution - locked in stresses - with the load measured during the load test);

The reasoning for these simplifying assumptions is to keep the method simple and straightforward for application in design, but it does not restrain future modifications within the same framework (that could be easily implemented).

In summary, the contributions of both end-bearing and shaft friction can be computed directly from the penetration force and the general formula for calculating the ultimate axial load capacity of the pile (Eq. 3) becomes:

$$Q_U = Q_L + Q_P = \frac{0.2U}{a_l}\sum F_d \Delta L + 0.7 F_d \frac{A_p}{a_p} \qquad (6)$$

The 0.2 value in Eq. 6 accounts for scale effects. In this general formula, a dynamic force is used to compute the static long term capacity of a pile which implies on disregarding visco-effects and pore-water pressures generated during the dynamic penetration of the sampler. As in all SPT-based methods ignoring these effects may induce errors in low permeable soils such as clays and silts. Since design procedures mainly involve considering the long term pile capacity, SPT data can be generally applied to sands, non-cohesive granular soils and most residual soil formations.

3. Database

An extensive search in the literature was conducted by Langone (2012) to identify instrumented pile load test publications with SPT penetration soundings adjacent to tested piles. A database of 89 instrumented incremental static load tests in different soil formations has been carefully reviewed in order to evaluate their suitability for the current research, considering availability of proper documentation on the pile data (installation and testing), subsurface exploration and general geotechnical laboratory and *in situ* testing data. Although all piles were subjected to static load tests, the loading procedure changed considerably reflecting local practice and standards, introducing errors and uncertainties to the overall analysis.

The ultimate axial load capacity for each pile was determined using the criterion recommended by the Brazilian Standard NBR 6122:2010, as illustrated in Fig. 1. Tests were chosen for their high degree of mobilization of pile capacity and the availability of reliable load-settlement relationships. However in several cases the *Vander der Veen* method (1953) had to be used to extrapolate the measured load-settlement curve of pile load tests that have not reached the required displacement of D/30 plus the elastic deformation of the pile.

Besides the proposed method, other semi-empirical and theoretical methodologies were employed for comparison purposes. The semi-empirical methods reflect the Brazilian engineering practice of foundation design: Aoki & Velloso (1975) and Décourt & Quaresma (1978). Since these methods were developed in Brazil, the energy efficiency is assumed to be of the order of 75%.

The theoretical approach uses bearing capacity theory associated with cavity expansion (Vésic, 1972). Vesic's approach to cavity expansion applied to cohesive-friction soils introduces some minor errors to the analysis because it does not consider the effect of cohesion in inhibiting dilation, as demonstrated by Mantaras & Schnaid (2002) and Schnaid & Mantaras (2003).

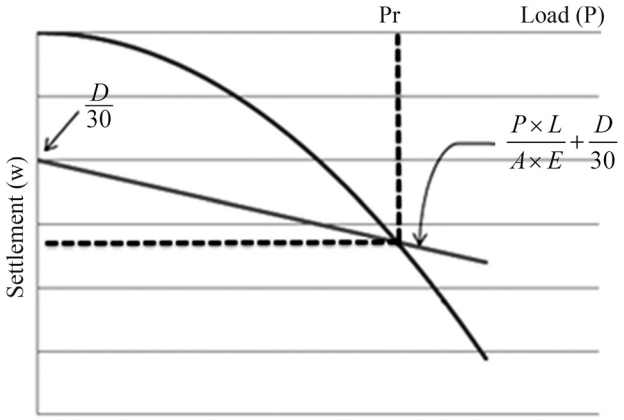

Figure 1 - Ultimate load based on the Brazilian Standard NBR 6122:2010.

When laboratory tests or soil parameters were not reported, SPT correlations were employed to estimate the friction angle (ϕ) and the Clam-Clay model ($S_u = 0.25\ \sigma'_v$) used to estimate the undrained shear strength.

4. Prediction and Performance

The ultimate axial load capacity of the pile predicted by dynamic penetration methods (Q_U) is compared to the measured pile capacity as obtained from the instrumented pile load tests using the Brazilian NBR 6122 failure criterion. By doing so, the predictive performance is presented and discussed. A summary of essential information related to the pile tests is shown in Table 1, including the pile size, type, length, location of the load test, the measured and predicted ultimate axial load capacity.

Initially the analysis concentrates on driven piles. End-bearing capacity (Q_P) and shaft friction capacity (Q_L) are computed from the measured data, as illustrated in Fig. 2 for a load test carried out in Brazil and reported by Falconi & Perez, (2008). This figure presents the load-settlement curve measured at the pile head and the actual load distribution along the pile at the final loading stage, as well as the SPT profile representative of ground conditions. The subsoil consists of a superficial 10 m thick fine silty sand layer, medium to dense, overlain a thick soft to very soft marine silty clay. Residual soil is encountered below 51 m depth. The tested H-pile was instrumented by strain gages placed at selected levels to determine the load distribution for each load applied to the pile head. Comparisons of measured and predicted loads cover the 4 methods used as reference in the present study. In this particular case, the the proposed method and the theoretical approach slightly underestimate the skin friction distribution whereas the semi- empirical methods overestimate the measured data.

Once the interpretation of each load test was completed, the measured and predicted values of Q_P, Q_L and Q_U were directly compared, as shown in Figs. 3, 4 and 5, respectively. In steel driven pile predictions, a limiting value of $N_{60} \leq 100$ was arbitrarily adopted.

Important observations derived from analysis can be summarized as follows:

- The proposed method predicts measured capacity values that are in general agreement with Brazilian practice;
- As previously stated, the method relies entirely on wave propagation and energy conservation, requiring a single empirical factor to account for scale effects;
- The arithmetic average and standard deviation of *measured* Q_m and *predicted* Q_P, Q_L and Q_U are indicators of the accuracy and precision of the prediction method. The proposed approach with average (QL/Qm) = 0.64 and deviation = 0.30 shows conservative estimated skin friction values with the lowest deviation when compared to other methods. Although Q_P is highly scattered, with average (QP/Qm) = 1.85 and deviation = 1.52, ultimate loads with average (QU/Qm) = 0.96 and deviation = 0.47 gives the best estimates. More importantly, in the proposed approach scatter could be reduced in the future by calibrating the SPT to derive local η efficiency factors (since average values have been used in the present analysis);

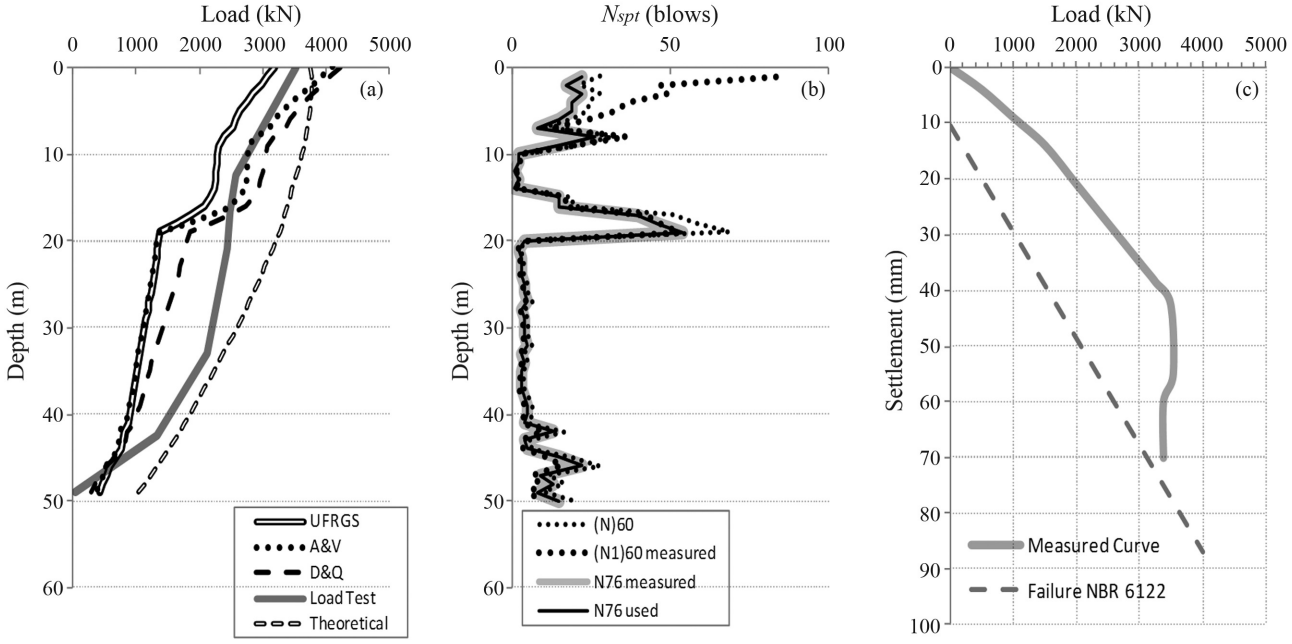

Figure 2 - Instrumented pile load test (a) predicted and measured load distribution (b) SPT profiles (c) load-settlement curve (adapted from Falconi & Perez, 2008).

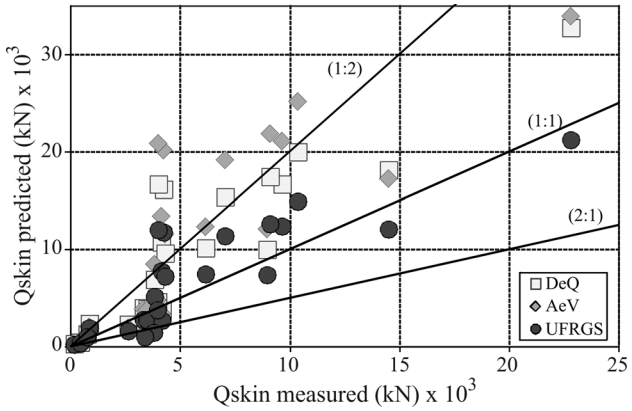

Figure 3 - Comparison of measured and predicted skin friction for steel piles.

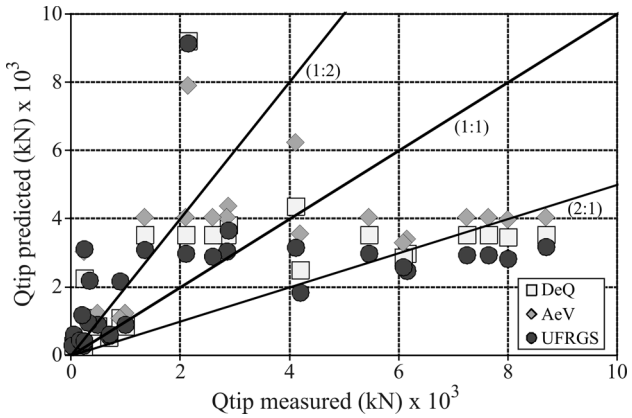

Figure 4 - Comparison of measured and predicted tip resistance for steel piles.

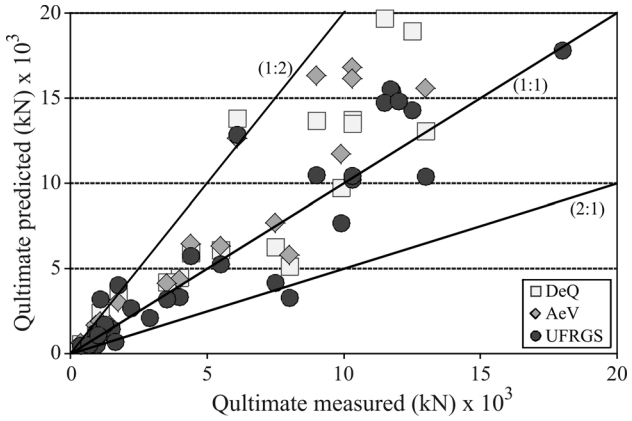

Figure 5 - Comparison of measured and predicted ultimate load for steel piles.

- The predictions of shaft resistance are much less scattered than predictions of end-bearing resistance. Errors in interpreting the measured values of end-bearing may be attributed to misleading evaluation of closed and open-ended piles, as well as the insufficient displacements at the pile tip during load tests to mobilize full end-bearing resistance;
- The proposed method shows no apparent bias of measured and predicted data with pile length (L), pile diameter (D), pile aspect ratio (L/D) and (more importantly) soil type. The principle of energy conservation combined to wave propagation analysis captures the influence of soil type.

5. Other Pile Types

The shaft friction and end-bearing resistance that can be developed on a pile are essentially related to the method of installation that dictates the magnitude of soil displacements and mobilized effective radial stresses. Embed on predicting the response of driven steel piles there is the assumption that q_p and f_l strongly correlates with F_d (or N_{spt}) since the mechanism of penetration, the large mobilized displacements imparted during installation and the interface friction angle shown some degree of similarity. Therefore variations in pile capacity developed by concrete driven piles, bored piles and continuous flight auger piles cannot be assessed from the same penetration measurement (being a SPT, LPT or CPT).

Extension of the approach to pile types other than driven steel piles requires two empirical factors, one for a proper evaluation of mobilized shaft friction and another for mobilized end bearing resistance:

$$Q_U = \alpha Q_L + \beta Q_P = \alpha \frac{0.2U}{a_l} \sum F_d \Delta L + 0.7 \beta F_d \frac{A_p}{a_p} \qquad (7)$$

where α and β are the pile type coefficients listed in Table 2 established from linear regression analysis (Lobo, 2005; Langone, 2012). Driven steel piles adopted as reference due to their similarity to SPT sampler penetration are represented by unitary values of α and β. Considering penetration restrain in hard layers and SPT reliability in case of discrete anomalies (localized high penetration values), the N_{spt} was arbitrarily limited according to values listed in Table 3.

Measured and predicted Q_P, Q_L and Q_U values are compared in Figs. 6 to 14 for precast concrete driven piles, bored piles and continuous flight auger piles. The following general conclusions can be drawn:

- *Precast concrete driven piles* have higher α coefficient than steel piles, reflecting the different nature of pile-soil friction interface. On average, predicted values of skin friction are of the same order of magnitude of measured loads, but slightly on the conservative side, *i.e.* predicted loads fall below the 1:1 best fit line for the predicted/measured pile capacities;
- Pedicted values of tip resistance show considerable scatter and a tendency to overestimate the measured resistance. Although this comparison may induce β values slightly lower than 1.1, the proposed value is justified by

Table 1 - Summary of instrumented steel pile test data.

Ref. / Fig.	Pile		Measured			UFRGS method						W_l/W_{ult}	Observations	Similarity	Reference	Average N_{60} (Shaft)	Average N_{60} (point)	Shaft material	Tip material
						Predicted			Predicted/Measured										
	L	Φ	Qskin	Qtip	Qult	Qskin	Qtip	Qult	Qskin	Qtip	Qult								
1	48	0.30	3299	701	4000	2785	568.3	3354	0.8	0.8	0.8	0.6	H, variable section, SML, BRA		Gerdau, not published	11	18	MULT	silty sand
2	7	0.36	435	495	930	333.4	904.3	1238	0.8	1.8	1.3	2.4	OP, SML, residual loads considered, EUA	A	Paik *et al.*, 2003	14	22	gravelly sand	gravelly sand
3	49	0.31	3490	40	3530	2758	431.6	3190	0.8	10.8	0.9	1.6	H, variable section, QML, BRA		Falconi & Perez, 2008	10	12	MULT	RS sandy silt
4	9	0.27	154,9	225,2	380	195.8	285.1	480.9	1.3	1.3	1.3	1.5	CP, η_1 = 40%, EUA		Briaud & Tucker, 1989	8	10	sand	sand
5	7	0.36	455	995	1450	333.4	904.3	1238	0.7	0.9	0.9	2.5	CP, SML, residual loads considered, EUA	A	Paik *et al.*, 2003	13	22	gravelly sand	gravelly sand
6	17	0.35	845	905	1750	1870	2177	4047	2.2	2.4	2.3	2.3	H, SML, residual load considered, EUA		Seo *et al.*, 2009	20	69	MULT	silty clay
7	55	0.43	4148	6152	10300	7720	2486	10206	1.9	0.4	1.0	0.8	H, SPT extrap., CHN	B	Yu, 2008	37	145	RS silty sand	RS silty sand
8	40	0.45	3813	6088	9900	5097	2580	7677	1.3	0.4	0.8	1.3	H, SPT extrap., CHN	B	Yu, 2008	27	94	RS silty sand	RS silty sand
9	80	1.50	22800	16200	39000	21230	35657	56887	0.9	2.2	1.5	1.0	OP, QML, SPT extrap, JPN	C	Kikuchi, *et al.*, 2007	23	68	clay + sand	sand
10	66	1.50	14500	16000	30500	12041	38445	50486	0.8	2.4	1.7	1.3	OP, QML, SPT extrap, JPN	C	Kikuchi, *et al.*, 2007	15	68	clay	sand
11	36	0.61	4160	240	4400	2640	3117	5757	0.6	13.0	1.3	1.1	conical toe, TWN, QML, residual loads considered		Yen, 1989	13	30	sand+clay	sand
12	33	0.61	2620	2880	5500	1577	3666	5243	0.6	1.3	1.0	0.1	CP, SINGAPORE		Moh, 1994	8	43	sand	silty sand
13	15	0.70	3961	2139	6100	3717	9127	12844	0.9	4.3	2.1	0.5	OP, BRA		Lopes, 1986	34	71	MULT	silty sand
14	41	0.60	3800	4200	8000	1428	1842	3270	0.4	0.4	0.4	0.4	OP, bitumen 26.0 m, JPN	D	Gyoten *et al.*, 1982	7	20	sand+clay	MUL
15	38	0.60	3380	4120	7500	1016	3155	4171	0.3	0.8	0.6	0.4	OP, bitumen 26.0 m, JPN	D	Gyoten *et al.*, 1982	16	42	sand+clay	MUL
16	17	0.36	755	345	1100	1008	2183	3191	1.3	6.3	2.9	2.8	CP, EUA		Kim *et al.*, 2009	20	87	MULT	silty clay
17	52	0.37	9655	2100	11755	12389	2985	15374	1.3	1.4	1.3	1.0	H, SPT extrap., residual loads considered, HKG	E	Zhang & Wang, 2007	61	118	MULT sand	RS silty sand
18	45	0.37	8950	1350	10300	7345	3084	10429	0.8	2.3	1.0	1.0	H, SPT extrap., residual loads considered, HKG	E	Zhang & Wang, 2007	36	118	MULT sand	RS silty sand
19	48	0.37	6150	2850	9000	7451	3042	10493	1.2	1.1	1.2	1.2	H, SPT extrap., residual loads considered, HKG	E	Zhang & Wang, 2007	35	118	MULT sand	RS silty sand
20	59	0.37	9100	2600	11700	12606	2885	15491	1.4	1.1	1.3	1.0	H, SPT extrap., residual loads considered, HKG	E	Zhang & Wang, 2007	53	118	MULT sand	RS silty sand
21	39	0.37	4300	8700	13000	7232	3169	10400	1.7	0.4	0.8	1.0	H, SPT extrap., residual loads considered, HKG	E	Zhang & Wang, 2007	41	118	MULT sand	RS silty sand
22	56	0.37	4250	7250	11500	11775	2928	14703	2.8	0.4	1.3	0.7	H, SPT extrap., residual loads considered, HKG	E	Zhang & Wang, 2007	48	118	MULT sand	RS silty sand
23	53	0.37	7050	5450	12500	11324	2971	14295	1.6	0.5	1.1	0.8	H, SPT extrap., residual loads considered, HKG	E	Zhang & Wang, 2007	55	118	MULT sand	RS silty sand
24	60	0.37	4000	8000	12000	11977	2831	14808	3.0	0.4	1.2	0.7	H, SPT extrap., residual loads considered, HKG	E	Zhang & Wang, 2007	39	79	MULT sand	RS silty sand
25	56	0.37	10350	7650	18000	14861	2928	17789	1.4	0.4	1.0	0.4	H, SPT extrap., residual loads considered, HKG	E	Zhang & Wang, 2007	69	118	MULT sand	RS silty sand

W_{ult} = settlement at ultimate load (mm). SML = slow maintain load. CP = closed pipe pile. Loads in kN.
W_{lt} = load test maximum settlement (mm). QML = quick maintain load. OP = opened pipe pile. Dimensions in meters.
H = "H" section pile. SPT extrap. = extrapolated SPT. MULT = multilayered soil. RS = residual soil.

back-analysis of non-instrumented load tests (Lobo, 2007) and by the fact that the measured value may not truly represent the ultimate resistance given the large displacements required for full mobilization;

- *Bored piles* mobilize the lowest α and β coefficients when compared to other pile types, due to stress relieving

Table 2 - Coefficients α and β for pile bearing capacity analysis.

Pile type	α	β
Precast concrete driven pile	1.5	1.1
Steel driven pile	1.0	1.0
Continuous flight auger pile	1.0	0.6
Bored pile	0.7	0.5

Table 3 - N_{spt} limits.

Pile type	N_{60} limits	
	Shaft region	Tip region
Precast concrete driven pile	30	50
Steel driven pile	100	100
Continuous flight auger pile	50	50
Bored pile	50	50

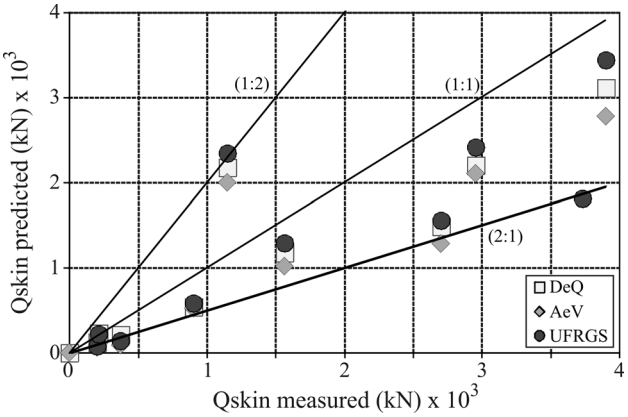

Figure 6 - Comparison of measured and predicted skin friction for precast concrete piles.

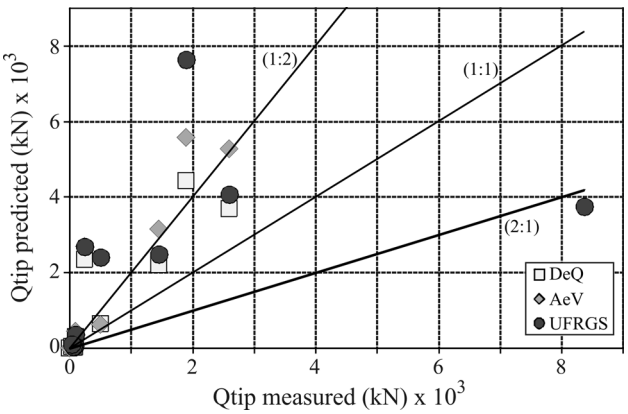

Figure 7 - Comparison of measured and predicted tip resistance for precast concrete piles.

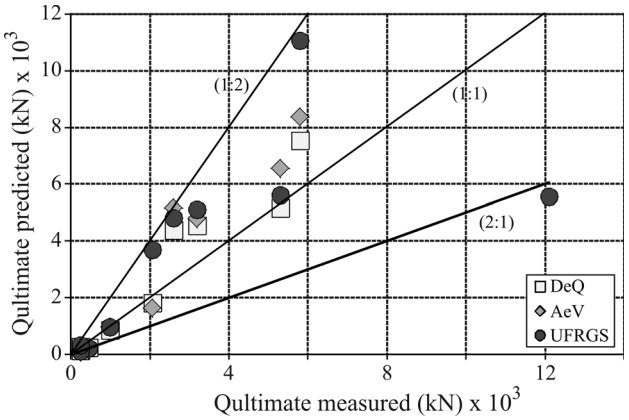

Figure 8 - Comparison of measured and predicted ultimate load for precast concrete piles.

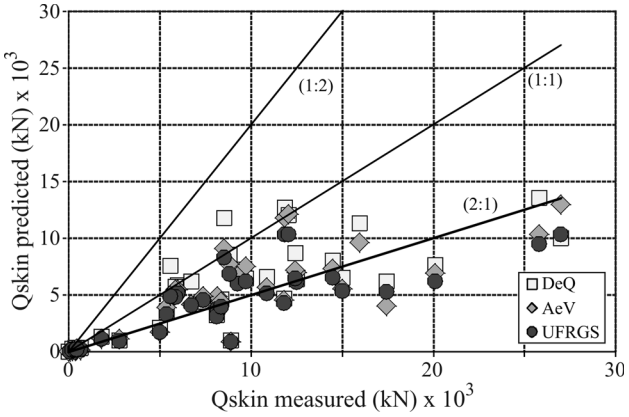

Figure 9 - Comparison of measured and predicted skin friction for bored piles.

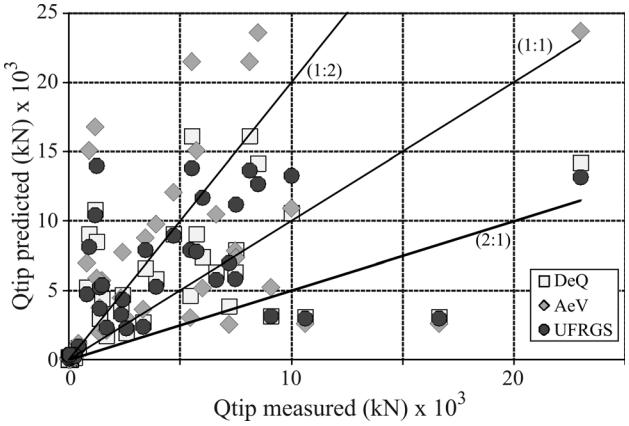

Figure 10 - Comparison of measured and predicted tip resistance for bored piles.

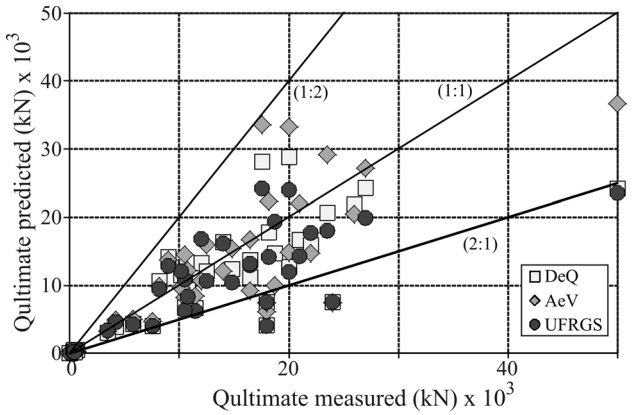

Figure 11 - Comparison of measured and predicted ultimate load for bored piles.

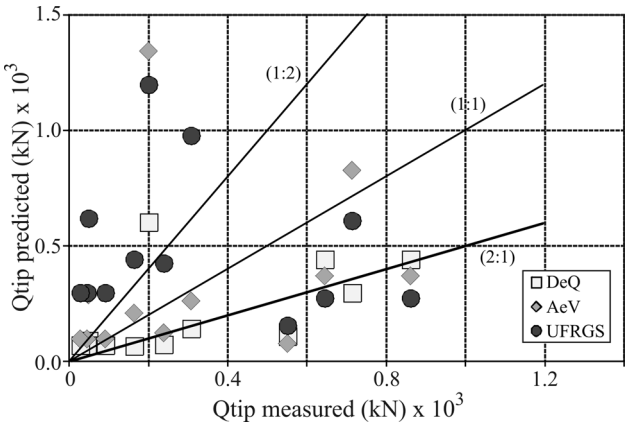

Figure 13 - Comparison of measured and predicted tip resistance for CFA piles.

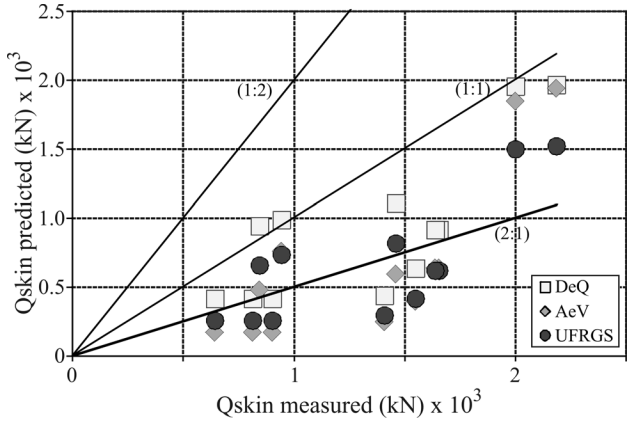

Figure 12 - Comparison of measured and predicted skin friction for CFA piles.

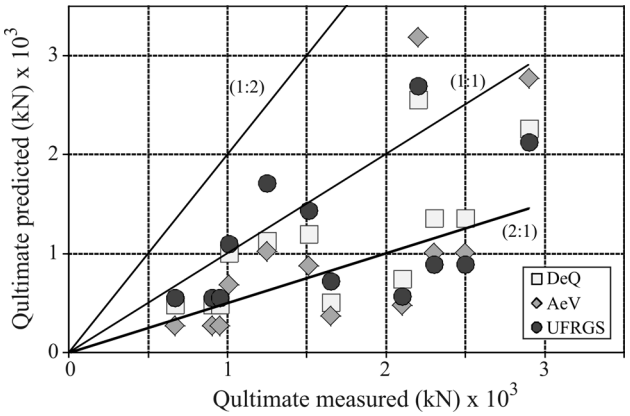

Figure 14 - Comparison of measured and predicted ultimate load for CFA piles.

induced by the excavation process. In average predicted skin friction underestimates measured values and tip resistance is scattered. Measured and predicted ultimate loads show good agreement;

- *Continuous flight auger piles*, *CFAP*, produce an intermediate condition between driven and bored piles. Although the α value of steel and CFA piles is the same, it does not necessarily represent similar pile-soil friction, because the oversupply of concrete or grout, and the consequent increase in diameter of CFAP, is disregarded in the analysis. In general predicted skin friction underestimates measured values and tip resistance is scattered. The proposed method is slightly conservative yielding predicted ultimate loads lower than measured.

In all predictions, the proposed method yields skin and tip resistance values within the range predicted by empirical methods classically adopted in Brazilian engineering practice. Predicted values generally lay around the best fit line for the predicted/measured pile capacities but, more importantly, for the database of instrumented load tests the method show the highest statistical probability of predicting values within 0.5*Qult* to 2*Qult* range. In addition, it is stressed that there is room for reducing scatter of predicted axial bearing capacity in a rational approach by calibrating energy efficiency coefficients to local SPT configurations.

6. Conclusions

This paper describes a new method developed for predicting the axial bearing capacity of individual piles, showing the strong relationship between the applied energy to SPT penetration test, its dynamic force and the ultimate resistance of steel driven piles. The method relies on energy conservation principles, wave propagation analysis and a number of hypotheses regarding the penetration mechanism. The main conclusions that can be drawn from the current analysis are:

- The method provides a valuable means of estimating the response of driven steel piles without having to rely on empirical statistical type of analysis;
- The proposed method can be extended to precast concrete driven piles, bored piles and continuous flight au-

ger piles, but empirical coefficients are necessary to account for the method of installation;

- Tthere appears to be room for reducing scatter of predicted axial bearing capacity by a proper calibration of energy efficiency coefficients representing the different configurations used in dynamic penetration tests;
- The proposed method shows no apparent bias of measured and predicted data with soil type, pile length (L), pile diameter (D), pile aspect ratio (L/D). Clearly the principle of energy conservation combined to wave propagation analysis captures the influence of soil type on the predicted values of axial bearing capacity;

These evidences and recommendations are supported by a final, overall picture given in Figs. 15 to 17, in which predicted/measured Q_P, Q_L and Q_U pile capacity values for driven, bored and continuous flight auger piles are simultaneously compared. The comparison to other established methods demonstrate the capability of the proposed SPT method in predicting the bearing capacity of piles: the method has been fully tested and is ready to be used in daily foundation design.

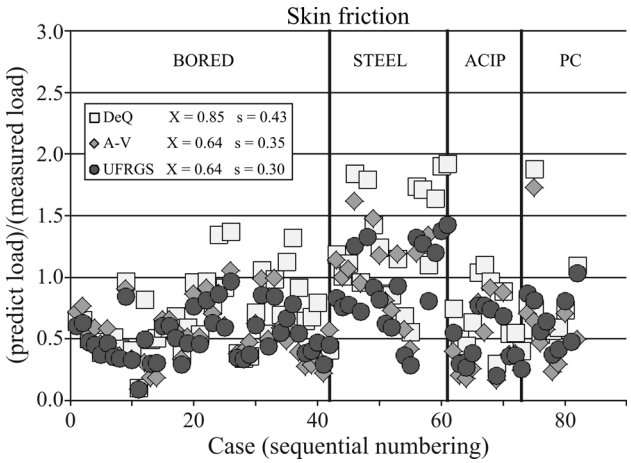

Figure 15 - Predictions of skin friction (after statistical cuts).

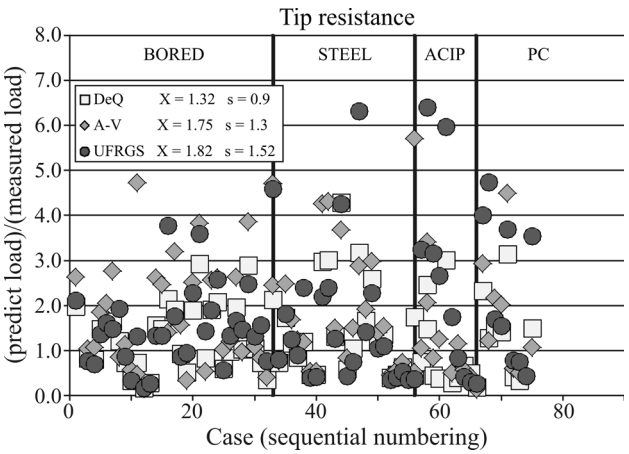

Figure 16 - Predictions of end bearing capacity (after statistical cuts).

Table 4 - Average and standard deviation of predictions (no statistical cuts).

		Predicted/measured							
		Proposed method		Aoki-Velloso		Décourt-Quaresma		Theoretical approach	
Pile type	Analysed aone	Average	SD	Average	SD	Average	SD	Average	SD
Steel	Skin friction	0.5	0.2	0.6	0.2	0.7	0.3	0.8	0.5
	Toe resistance	2.7	3.1	2.5	3.4	2.2	2.4	9.0	10.4
	Failure	0.8	0.3	0.8	0.4	0.8	0.3	2.0	1.0
Bored	Skin friction	1.2	0.7	1.9	1.2	1.7	0.9	0.7	0.4
	Toe resistance	2.3	3.2	2.4	2.8	2.0	2.2	3.2	5.8
	Failure	1.2	0.5	1.7	0.5	1.5	0.5	1.0	0.5
ACIP	Skin friction	0.5	0.2	0.5	0.3	0.7	0.3	0.5	0.1
	Toe resistance	4.0	4.1	2.0	2.2	1.0	0.9	10.4	10.6
	Failure	0.7	0.4	0.6	0.4	0.7	0.3	1.2	0.5
PC	Skin friction	0.8	0.5	0.7	0.4	0.8	0.4	0.6	0.4
	Toe resistance	3.2	3.1	2.9	3.3	2.4	2.8	4.5	3.5
	Failure	1.2	0.6	1.0	0.6	1.0	0.4	1.3	0.5

SD: Standard deviation.

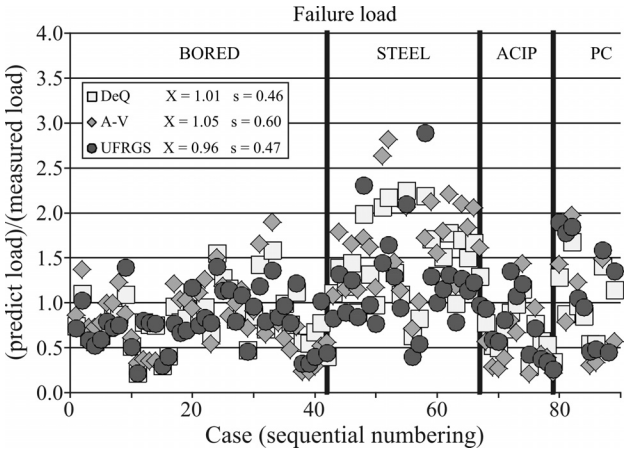

Figure 17 - Predictions of ultimate axial load capacity (after statistical cuts).

Acknowledgments

The writers wish to express their gratitude to the Federal University of Rio Grande do Sul, as well as to the Brazilian Research Council for the financial support to the research project and to the research group.

References

Aoki, N. & Velloso, D.A (1975) An approximate method to estimate the bearing capacity of piles. Proc. Panamerican Conference on Soil Mechanics and Foundation Engineering, Buenos Aires ISSMGE, pp. 116-127.

Axelsson, G. (1998) Long-term increase in shaft capacity of non-cohesive soils. M.Sc. Thesis, Royal Institute of Technology, Division of Soil and Rock Mechanics, Stockholm, 122 p.

Bazaraa, A.R. & Kurkur, M.M. (1986) N-values used to predict settlements of piles in Egypt. In: Use of In Situ Tests in Geotechnical Engineering. ASCE Geotechnical Special Publication n. 6, p. 462-47.

Briaud, J.L. & Tucker, L.M. (1988) Measured and predicted axial response of 98 Piles, Journal of Geotechnical Engineering, ASCE, v.114:9, p. 984-1001.

Briaud, J.L.; Tucker, L.M. & Ng, E. (1989) Axially loaded 5 pile group and single pile in sand. Proc. 12th International Conference of Soil Mechanics and Foundation Engineering, Rio de Janeiro, pp. 1121-1124.

Bustamante, M. & Gianeselli, L. (1982) Pile bearing capacity predictions by means of static penetrometer CPT. Proc. The Second European Symposium on Penetration Testing. 24-27 May, Balkema, Amsterdam, v. 2, p. 493-500.

Dalla Rosa, S. (2008) Study of Scale Effects in Dynamic Penetrarion Tests. M.Sc. Thesis, Programa de Pós-Graduação em Engenharia Civil, Universidade Federal do Rio Grande do Sul, 173 p. (in Portuguese).

Décourt, L. & Quaresma, R.A. (1978) Capacidade de carga de estacas a partir de valores de SPT. Anais do Congresso Brasileiro de Mecânica dos Solos e Engenharia de Fundações, Rio de Janeiro, ABMS, Rio de Janeiro, pp. 45-53.

De Mello, V.F.B. (1971) The standart penetration test state-of-the-art report. Proc. 4th Panamerican Conference on Soil Mechanics and Foundation Engineering, San Juan, pp. 1-86.

De Nicola, A. & Randolph, M.F. (1993) Tensile and compression shaft capacity of piles in sand. Journal of Geotechnical Engineering, ASCE, v. 119:12, p. 1952-1973.

De Ruiter, J. & Berigem, F.L. (1979) Pile foundation for large north sea structures. Marine Geotechnology, v.3:3, p. 276-314.

Falconi, F.F. & Perez Júnior, W. (2008) Estacas metálicas profundas de seção decrescente na Baixada Santista - Complemento aos estudos anteriores com base em novas provas de carga. Proc. Congresso Brasileiro de Mecânica dos Solos e Engenharia de Fundações, Búzios, ABMS/ABEF, São Paulo, CD -Rom.

Gyoten, Y.; Mizuhata, K. & Fukusumi, T. (1982) Tests on full-sized piles driven in reclaimed land. Soils and Foundations, Tokyo, v. 22:4, p. 81-95.

Jardine, R.; Chow, F., Overy, R. & Standing, J. (2005) ICP Design Methods for Driven Piles in Sands and Clays. Thomas Telford, London.

Jardine, R.J.; Standing, J.R. & Chow, F.C. (2005a) Field research into the effects of time on the shaft capacity of piles driven in sand. Proc. International Symposium on Frontiers in Offshore Geotechnics, Perth, Taylor & Francis.

Kikuchi, Y.; Mizutani, M. & Yamashita H. (2007) Vertical bearing capacity of large diameter steel pipe piles. Proc. Advances in Deep Foundations. International Workshop on Recent Advances of Deep Foundations, Yokosuka, Japan. Taylor & Francis, London, pp. 177-182.

Kim, D.; Bica, A.V.D.; Salgado, R. & Prezzi, M. (2009) Loading testing of a closed-ended pipe pile driven in multilayered soil. Journal of Geotechnical and Geoenvironmental Engineering, ASCE, v. 135:4, p. 463-473.

Langone, M.J. (2012) Método UFRGS de Previsão de Capacidade de Carga em Estacas: Análise de Provas de Carga Estáticas Instrumentadas. M.Sc. Thesis in Engineering, Programa de Pós-Graduação em Engenharia Civil, Universidade Federal do Rio Grande do Sul, 152 p.

Lehane, B.M.; Jardine, R.J.; Bond, A.J. & Frank, R. (1993) Mechanisms of shaft friction in sand from instrumented pile tests. Journal of Geotechnical Engineering, ASCE, v. 119:1, p. 19-35.

Lehane, B.M.; Schneider, J.A. & Xu, X. (2005) The UWA-05 method for prediction of axial capacity of

driven piles in sand.Proc. International Symposium on Frontiers in Offshore Geotechnics. Perth, A.A. Balkema, pp. 683-689.

Lehane, B.M.; Schneider, J.A. & Xu, X. (2007) Development of the UWA-05 design method for open and closed ended driven piles in siliceous sand. Proc. GeoDenver, New Peaks in Geotechnics, pp. 157-174.

Lobo, B.O. (2005) Método de Previsão de Capacidade de Carga de Estacas: Aplicação dos Conceitos de Energia do Ensaio SPT. M.Sc. Thesis in Engineering, Programa de Pós-Graduação em Engenharia Civil, Universidade Federal do Rio Grande do Sul, 121 p.

Lobo, B.O. (2009) Dynamics Penetration Mechanics in Cohesionless Soils. PhD Dissertation in Engineering, Programa de Pós-Graduação em Engenharia Civil, Universidade Federal do Rio Grande do Sul, 225 p.

Lobo, B.O.; Schnaid, F.; Odebrecht, E. & Rocha, M.M. (2009) Previsão de capacidade de carga de estacas através dos conceitos de energia do Ensaio SPT, Geotecnia, v. 115, p. 5-20.

Lopes, F.R. (1986) Medições de transferência de carga em estacas. Proc. Congresso Brasileiro de Mecânica dos Solos e Engenharia de Fundações, ABMS/ABEF, Porto Alegre, v. 8. p. 25-42.

Mantaras, F.M. & Schnaid, F. (2002) Cylindrical cavity expansion in dilatant cohesive-frictional materials. Geotechnique, v. 52:5, p. 337-348.

Moh, Z.C. (1994) Current deep foundation practice in Taiwan and Southeast Asia. Proc. International Conference on Design and Construction of Deep Foundations, FHWA, Orlando, p. 1137-1161.

Odebrecht, E.; Schnaid, F.; Rocha, M.M. & Bernardes, G.P. (2005) Energy efficiency for standard penetration tests. Journal of Geotechnical and Geoenvironmental Engineering, ASCE, v. 131:10, p. 1252-1263.

Paik, K.; Salgado, R.; Lee, J. & Kim, B. (2003) Behavior of open and closed ended piles driven into sands. Journal of Geotechnical and Geoenvironmental Engineering, ASCE, v. 129:4, p. 296-306.

Schnaid, F. (2000) Ensaios de Campo e suas Aplicações na Engenharia de Fundações. São Paulo, Oficina de Textos, p. 189.

Schnaid, F. (2005) Geocharacterisation and properties of natural soil by in situ tests. Proc. The 16th International Conference on Soil Mechanics and Geotechnical engineering, v. 1, p. 3-46.

Schnaid, F. & Mantaras, F.M. (2003) Cavity expansion in cemented materials: Structure degradation effects. Geotechnique, v. 53:9, p. 797-807.

Schnaid, F.; Odebrecht, E. & Rocha, M.M. (2007) On the mechanics of dynamic penetration test. Geomechanics and Geoengineering: An International Journal, v. 2:2 p. 137-146.

Schnaid, F. & Yu, H.S. (2007) Theoretical interpretation of the seismic cone test in granular soils. Geotechnique, v. 57:3, p. 265-272.

Schnaid, F. & Odebrecht, E.; Rocha, M.M. & Bernardes, G.P. (2009) Prediction of soil properties from the concepts of energy transfer in dynamic penetration tests. Journal of Geotechnical and Geoenvironmental Engineering, ASCE, v. 135:8.

Seo, H.; Yildirim, I.Z. & Prezzi, M. (2009) Assessment of the axial load response of an h pile driven in multilayered soil. Journal of Geotechnical and Geoenvironmental Engineering, ASCE, v. 135:12, p. 1789-1804.

Skempton, A.W. (1986) Standard penetration test procedures and the effects in sands of overburden pressure, relative density, particle size, ageing and overconsolidatin. Géotechnique, v. 36:3, p. 425-447.

Vesiæ A.S. (1972) Expansion of cavities in infinite soil mass. Journal of the Soil Mechanics and Foundations Division: Proc. The American Society of Civil Engineers, ASCE, v. 98, n. SM3.

Xu, X. & Lehane, B.M. (2005) Evaluation of end-bearing capacity of closed-ended pile in sand from cone penetration data. In: International Symposium on Fronties in Offshore Geotechnics, Perth, Taylor & Francis p. 19-21.

Yen, T.L.; Lin, H.; Chin, C.T. & Wang, R.F. (1989) Interpretation of instrumented driven steel pipe piles. Proc. Foundation Engineering: Current Principles and Practices. Evanston, ASCE, New York, v. 2, pp. 375-392.

Yu, F. (2011) Field tests on instrumented h-piles driven into dense sandy deposits. Electronic Journal of Geotechnical Engineering, EJGE, v. 14, 2008. Available in , accessed in Sep. 4, 2011.

Zhang, L.M. & Wang, H. (2007) Development of residual forces in long driven piles in weathered soils. Journal of Geotechnical and Geoenvironmental Engineering, ASCE, v. 133:10, p. 1216-1228.